Desalination and Water Treatment
www.deswater.com
doi: 10.1080/19443994.2015.1012338

56 (2015) 2773–2780
December

Taylor & Francis
Taylor & Francis Group

Removal of methylene blue onto mineral matrices

Mohamed El Khames Saad[a], Najib Mnasri[a], Mohsen Mhamdi[a], Tarik Chafik[b], Elimame Elaloui[a,c], Younes Moussaoui[c,d,*]

[a]*Material Environment and Energy Laboratory (06/UR/12-01), Science Faculty of Gafsa, Gafsa University, Gafsa, Tunisia, Tel./Fax: +216 76210052; email: limam_aloui@yahoo.fr (E. Elaloui)*
[b]*Chemical Engineering and Resource Development Laboratory (UAE/L01FST), Sciences and Techniques Faculty of Tanger, University Abdelmalek Essaadi, BP 416, Tangier, Morocco, Tel. +212 539393954/55; Fax: +212 539393954; email: tchafik@yahoo.com*
[c]*Science Faculty of Gafsa, Gafsa University, Zarroug City 2112, Tunisia, Tel./Fax: +216 76210052; email: y.moussaoui2@gmx.fr*
[d]*Physical Organic Chemistry Laboratory (UR11-ES74), Science Faculty of Sfax, Sfax University, Sfax 3018, Tunisia, Tel. +216 74276400; Fax: +216 74274437*

Received 1 January 2014; Accepted 16 November 2014

ABSTRACT

The textile industry generates huge volumes of dye-contaminated wastewater. Discharging these effluents into the environment causes many diseases that can be detrimental to human health. Therefore, adsorption of these types of dyes such as methylene blue onto mineral matrices offers an efficient method for pollution remediation. The present investigation is undertaken to test the use of Tunisian clay in raw and sodium form to remove methylene blue from aqueous solution. The experimental data were analysed using the Langmuir, Freundlich, Temkin and Dubinin–Radushkevich isotherms. The equilibrium data fit well to the Langmuir model, and the monolayer adsorption capacity for methylene blue dye is 312.5 and 208.33 mg/g, respectively with sodium clay (MS002-1) and raw clay (MS001-2).

Keywords: Adsorption; Clay; Dye; Adsorption isotherm

1. Introduction

Recently, there are more than 10,000 synthetic dyes with different chemical structures and form (cationic, anionic and non ionic) that are commercially available [1–7]. These kinds of dyes are used by many industries such as textile, cosmetics, paint, papermaking and ceramic use in order to colour their products [8–10]. It is estimated that about 10–20% of the dyes were lost in industrial effluents during manufacturing or processing operations. However, the discharge of untreated and/or partially treated useful solutions containing large amounts of residuals dyes into municipal wastewater plants and/or environment may cause the formation of toxic carcinogenic breakdown products [11–13]. This dye-contaminated wastewater has the potential danger on human life as well as on environmental ecosystems [14,15]. In the last decades, the removal of synthetic organic dyestuff from wastewater becomes an environmental challenge [11,16]. Methylene blue is commonly one of cationic dyes, which has wide applications

---

*Corresponding author.

Presented at the 4th Maghreb Conference on Desalination and Water Treatment (CMTDE 2013) 15–18 December 2013, Hammamet, Tunisia

including colouring paper, dyeing cottons, wools, silk, leather and coating of paper stock. Although it is not strongly hazardous, methylene blue can cause permanent injury to human and animal eyes [17]. And, its removal from waste effluents is rather difficult because of its synthetic origins and stable chemical structures. Many technologies are employed to remove dye from aquatic environments, including anaerobic/aerobic treatment [18,19], coagulation/flocculation [20], oxidation/ozonation [10,21–23], membrane separation [24] and sorption [25–28]. The adsorption onto mineral clay has been found to be the effective technique in wastewater treatment methodology because of its wide capability of adsorption of different types of adsorbate, inexpensive and rapid/assisted design method.

In this study, we report the use of raw clay obtained from Oued Tfal, Gafsa, (south of Tunisia) and its sodium form as adsorbents for the removal of methylene blue from an aqueous solution.

2. Experimental

2.1. Materials and measurements

2.1.1. Methylene blue

Methylene blue (IUPAC name is 3,7-bis(dimethylamino)-phenothiazin-5-ium chloride) was chosen as a thiazine cationic dye, its molecular formula is $C_{16}H_{18}N_3SCl\text{-}3H_2O$, and its molecular weight is 373.9 g/mol, and the different resonance structures are given in Fig. 1.

2.1.2. Clay mineral

The raw clay (MS001-2) taken from Oued Tfal, Gafsa (South Tunisia) was used in this study. Its chemical composition was found to be: 51.3% SiO_2, 2.68% MgO, 10.26% Al_2O_3, 0.34% K_2O, 9.98% CaO, 3.57% F_2O_3, 1.32% Na_2O and 21.28% loss of ignition [29].

The sodium clay (MS002-1) was obtained from the raw clay as has been described previously [30]. The raw clay was suspended in bi-distilled water in order to collect the granulometric fraction size lower than 2 μm. Then, the obtained fraction was treated by 0.05 M HCl solution in order to destroy carbonates in the clay particles. Then, the solid phase was dispersed in 1 M of NaCl solution for 12 h. The supernatant chloride solution was removed and replaced by a fresh NaCl solution (1 M). This process was repeated four times. The sample was put into tubing dialysis membrane and placed in bi-distilled water to remove the chloride ions. Then, the water was changed daily until the absence of chloride ($AgNO_3$ test). After dialysis, the sample was dried at 70˚C and finally hand ground in an agate mortar to obtain particle size lower than 80 μm.

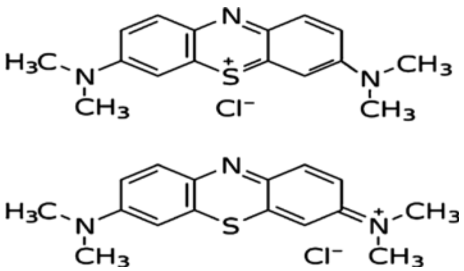

Fig. 1. Different resonance structures of methylene blue.

The raw and sodium clay powder was stored in a plastic bottle to be used later in the experiments.

2.1.3. Adsorbents characterisation

Several methods were used in this study to characterise the MS001-2 and MS002-1 clays.

X-ray diffraction (XRD) patterns of the samples were recorded between 5˚ and 80˚ 2θ ranging at a scanning speed of 2˚min, using X-ray a Philips goniometer, PW1730/10 instrument with Cu Ka radiation (40 kV, 30 mA, $\lambda = 0.15406$ nm).

The specific surface area and pore size distribution of the clay samples were made by nitrogen adsorption–desorption experiments at 77 K using a Micromeritics ASAP 2020C instrument. Before the measurement, clay samples were out gassed under a reduced atmosphere for 8 h at 110˚C. The specific surface area was determined according to the standard Brunauer–Emmett–Teller method [31], while the average pore diameter was determined directly from the isotherm by applying the Barrett–Joyner–Halenda (BJH) method.

2.2. Equilibrium adsorption experiments

The adsorption experiments were performed by batch experiments of 40 mg of sorbents (MS001-2 or MS002-1) with 10 mL methylene blue solution of known concentration and initial solution pH. The mixture was shaken at room temperature (25˚C) for specified time. Then, the suspensions were separated from the adsorbent by centrifugation and analysed using an UV–Vis spectrophotometer (BECKMAN DU 800) set at a wavelength of 664 nm.

The experiments were carried out by varying contact time and concentration of initial dye solution. Adsorption mechanisms were studied according to predefined procedure with methylene blue concentration ranging from 30 to 150 mg/L.

The equilibrium concentration of methylene blue and the adsorbed amount of dye, q_e (mg/g), were, respectively, calculated according to following equation,

$$C_e = (5.3053 \times A) - 0.2876 \tag{1}$$

$$q_e = \frac{(C_i - C_e) \times V}{W} \tag{2}$$

where A is the dye absorbance at 664 nm, q_e is the amount of dye adsorbed (mg/g). C_i and C_e are the initial and equilibrium concentrations of dye (mg/L), respectively. V is the volume of the solution (L), and W is the sorbent weight (g).

3. Results and discussions

3.1. XRD analysis

The X-ray diffractograms of samples shown in Fig. 2 gives the mineralogical composition of different phases.

XRD analysis of MS001-2 shows a main phase with a d_{001} at low theta value (1.47 nm), characteristic of a smectite type clay, and also illite (0.98 nm), kaolinite (0.71 nm), calcite (0.303 nm) and quartz (0.340 nm). After purification, the reflections corresponding to calcite and quartz were completely disappeared.

3.2. Nitrogen adsorption/desorption isotherm at 77 K

The textural properties of samples are obtained from the standard BET method and the BJH equation, respectively. The nitrogen adsorption/desorption isotherm at 77 K of MS001-2 and MS002-1 samples are shown in Fig. 3. According to the IUPAC classification, it is noted that the raw and sodium clay isotherm are of type II. A large uptake of nitrogen is observed close to the saturation pressure, exhibiting multilayer adsorption and implying the presence of mesopores [32]. Furthermore, the pores' size distribution (using the BJH method) (Fig. 4) shows that the diameters pores of each samples vary between 30 and 50 Å with a maximum distribution towards 38 Å, indicating the uniform mesoporous structures of these samples. The specific surface increases after purification process from 110 m^2/g for the raw clay (MS002-1) to reach 144 m^2/g for sodium clay (MS001-2).

3.3. Adsorption kinetics

The kinetics of adsorption is one of the most important characteristics in defining the efficiency of the adsorption process.

The pseudo-first-order (Eq. (3)) and pseudo-second-order (Eq. (4)) were applied to investigate the experimental data and the adsorption processes [33]. The goodness of fit of the equations to the data was evaluated based on the constant (R^2).

$$\ln(q_e - q_t) = \ln q_e - k_1 t \tag{3}$$

$$\frac{t}{q_t} = \frac{1}{k_2 q_e^2} + \frac{t}{q_e} \tag{4}$$

where q_e and q_t (mg/g) are the adsorption capacity at equilibrium and at time t, respectively, K_1 (1/min) and K_2 (g/(mg min)) are the rate constant of pseudo-first-order and pseudo-second-order adsorption, respectively.

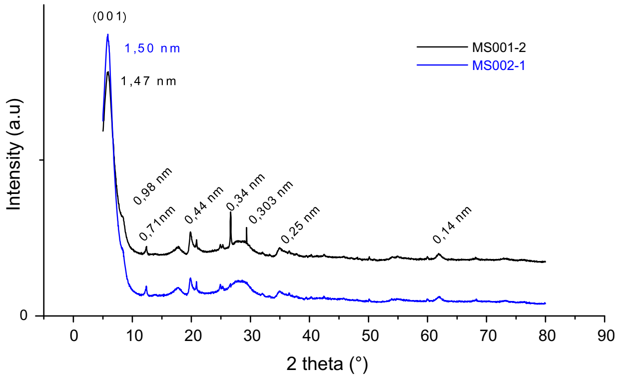

Fig. 2. XRD patterns of MS001-2 and MS002-1 samples.

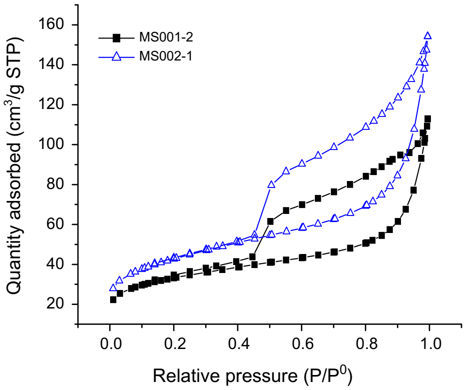

Fig. 3. Nitrogen adsorption/desorption isotherm at 77 K.

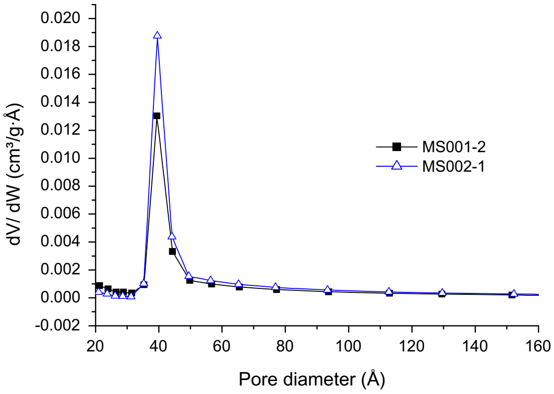

Fig. 4. BJH pore size distribution of clay samples.

Adsorption of MB dye by raw and sodium clay was investigated at different initial concentrations (40, 60 and 100 mg/L). Results showed a fast adsorption of MB during the first 10 min (Fig. 5). This result was ascribed to the large amount of adsorption sites available on adsorbents at the beginning of adsorption. Then, adsorption progresses slowly to become less efficient after 20 min due to the gradual saturation of adsorption sites on clays surface. The evolution of the adsorbed amount of MB onto the two types of adsorbents shows that equilibrium time was independent of the initial concentration, and the adsorbed MB at equilibrium was increased with increasing of initial concentration. This is due to the fact that the diffusion of MB molecules in solution to the surface of the adsorbent is accelerated by increasing the concentration of dye.

Kinetic constants and correlation coefficient of both pseudo-first-order and pseudo-second-order models of MB adsorption onto minerals materials were summarised in Table 1.

The correlation coefficient values (R^2) obtained for pseudo-first-order model are between 0.79 and 0.98. Furthermore, the calculated values $q_{e\cdot \text{cal}}$ are not in agreement with the experimental values showing that the adsorption kinetics did not follow the pseudo-first-order model. The extremely high correlation coefficients (R^2) and the agreements of calculated values $q_{e\cdot \text{cal}}$ of MB retention with the experimental data give a better description of the adsorption data by the pseudo-second-order model.

3.4. Adsorption isotherm

In order to study the theoretical aspects of MB adsorption onto raw and sodium clay, four models Langmuir, Freundlich, Temkin and Dubinin–Radushkevich (D–R) were used to fit the experimental data [34,35].

The Freundlich model was expressed by the nonlinear equation and the linear form as shown in following equations,

$$q_e = K_F \cdot C_e^{1/n} \tag{5}$$

$$\log q_e = \log K_F + (1/n) \log C_e \tag{6}$$

where q_e is the equilibrium amount of solute adsorbed per unit mass of adsorbent (mg/g), C_e is the equilibrium concentration of solute in bulk solution (mg/L), K_F is the Freundlich constant related to the adsorption capacity of adsorbent ((mg/g) $(\text{mg/L})^{1/n}$), and $1/n$ is the indication of the tendency of the adsorbate to be adsorbed.

The nonlinear and linear expressions of the Langmuir isotherm are respectively represented by the following equations.

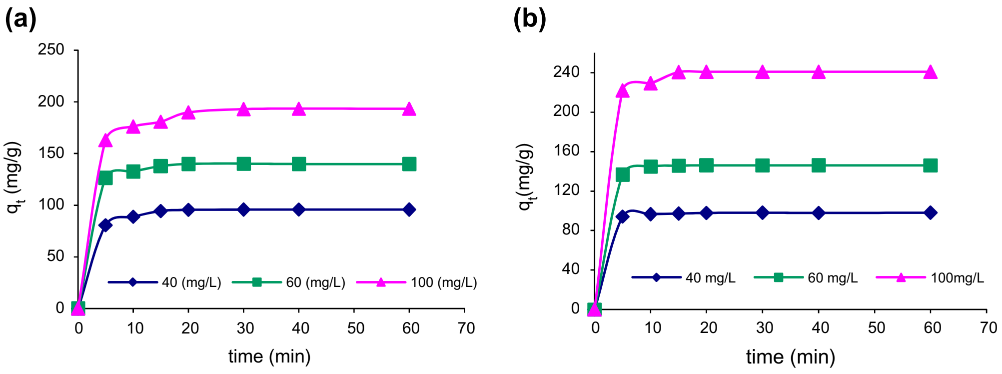

Fig. 5. Influence of the initial MB concentration on the adsorption process onto (a) raw clay and (b) sodium clay.

Table 1
Kinetic parameters for adsorption of MB onto mineral matrices

Concentration (mg/L)	$q_{e\ \mathrm{exp}}$ (mg/g)	Pseudo-first order			Pseudo-second order		
		$q_{e\ \mathrm{cal}}$ (mg/g)	$K_1\ 10^{-1}$ (1/min)	R^2	$q_{e,\ \mathrm{cal}}$ (mg/g)	$K_2\ 10^{-2}$ (g/(mg min))	R^2
MS001-2							
40	95.81	74.41	2.64	0.98	97.08	1.4	0.99
60	139.73	95.545	2.68	0.94	140.84	1.6	0.99
100	193.35	135.68	1.87	0.96	196.07	0.4	0.99
MS002-1							
40	97.89	86.04	2.86	0.79	98.03	6.5	1
60	146.17	49.78	2.77	0.88	147.05	3.8	1
100	240.86	114.06	2.95	0.89	243.90	1.2	0.99

$$q_e = \frac{q_{\max} \cdot K_L \cdot C_e}{1 + K_L \cdot C_e} \tag{7}$$

$$\frac{C_e}{q_e} = \frac{C_e}{q_{\max}} + \frac{1}{q_{\max} \cdot K_L} \tag{8}$$

where $q_{\max}$ is the maximal adsorption capacity (mg/g), and K_L is the constant related to free adsorption energy (L/mg) that is the reciprocal of the concentration at which half saturation of the adsorbent is reached.

Heat of adsorption and the adsorbent–adsorbate interaction on adsorption isotherms were studied by Temkin model. The nonlinear and the linear Temkin isotherm equation are given by the following equation [36].

$$q_e = \frac{\mathrm{RT}}{b_T} \ln\,(A_T C_e) \tag{9}$$

$$q_e = \frac{\mathrm{RT}}{b_T} \ln A_T + \left(\frac{\mathrm{RT}}{b_T}\right) \ln C_e \tag{10}$$

$$q_e = B \ln A_T + B\ \ln C_e \tag{11}$$

where A_T is Temkin isotherm equilibrium binding constant (L/g), b_T is the Temkin isotherm constant, R is the universal gaz constant (8.314 J/mol K), T is the temperature (K), B = RT/b_T is the constant related to heat of sorption (J/mol).

The Temkin isotherm equation assumes that the heat of adsorption of all the molecules in the layer decreases linearly with coverage due to adsorbent–adsorbate interaction, and that the adsorption is characterised by a uniform distribution of binding energies, up to some maximum binding energy.

The (D–R) model is useful to determine the adsorption type and it can be expressed as [37]:

$$q_e = q_s \exp(-k\xi^2) \tag{12}$$

$$\ln q_e = \ln\,(q_s) - (k\xi^2) \tag{13}$$

where k (mol^2/kJ^2) is the constant related to the adsorption energy, q_s is the theoretical isotherm saturation capacity (mg/g), and ξ is the D–R isotherm constant calculated by using following equation:

$$\xi = \mathrm{RT}\ \ln\left(1 + \frac{1}{C_e}\right) \tag{14}$$

where R is the gas constant (kJ/kmol), and T is the temperature (K).

Table 2
Constants of Langmuir, Freundlich, Temkin and D–R isotherms and the regression coefficients for adsorption of BM onto minerals matrices

	Langmuir			Temkin			
Parameters	$q_{\max}$ (mg/g)	K_L (L/mg)	R^2	B (J/mol)	A_T (L/g)	b_T	R^2
MS001-2	208.33	0.71	0.99	29.85	24.67	82.99	0.90
MS002-1	312.5	0.82	0.99	54.17	14.36	45.73	0.90
	Freundlich			D–R			
Parameters	K_F (mg/g) (L/mg)$^{(1/n)}$	$1/n$	R^2	q_s (mg/g)	K (mol^2/kJ^2)	E (kJ/mol)	R^2
MS001-2	86.45	0.24	0.80	191.36	0.20	1.56	0.95
MS002-1	134.36	0.29	0.81	261.83	0.17	1.68	0.92

The adsorption energy E (kJ/mol) is the free energy change when one mole of the ion is transferred to the surface of the solid from infinity in the solution. It can be defined by:

$$E = \frac{1}{\sqrt{2k}} \quad (15)$$

The results of the isotherm modelling studies and the regression coefficients, R^2, were used to evaluate the adsorption parameters and these parameters are given in Table 2. According to Table 2, the correlation coefficients values of the linear plot of Langmuir model are very high compared to those of Freundlich, Temkin and D–R model which were found less than 0.98. Experimental data of the adsorption of MB onto raw and sodium clay obey very well to the Langmuir model. The adsorption capacity of MB calculated from the Langmuir, Freundlich and D–R isotherm models onto sodium clay (MS002-1) is superior to the adsorption capacity onto the raw clay (MS001-2) (Table 2).

The essential characteristics of Langmuir adsorption isotherm can be expressed in terms of a dimensionless equilibrium constant [38], R_L, which can be defined by Eq. (16).

$$R_L = \frac{1}{1 + K_L \cdot C_i} \quad (16)$$

The R_L contributes to predict whether the adsorption process is favourable or unfavourable. The calculated values of R_L for raw ($0.009 < R_L < 0.06$) and sodium clay ($0.008 < R_L < 0.03$) were all between 0 and 1, it can be concluded that the adsorption of MB occurred favourable with the two types of adsorbents.

The experimental data of MB adsorption onto raw and sodium clay are in harmony with the Langmuir model as shown in Figs. 6 and 7. The maximum adsorption capacity of MB onto raw and sodium clay consists of a monolayer adsorption and the adsorbents sites are energetically identical.

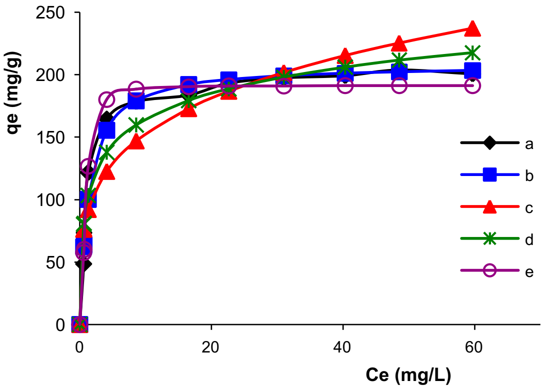

Fig. 6. Adsorption isotherm of MB onto MS001-2: (a) experimental, (b) Langmuir fit, (c) Freundlich fit, (d) Temkin fit and (e) D–R fit.

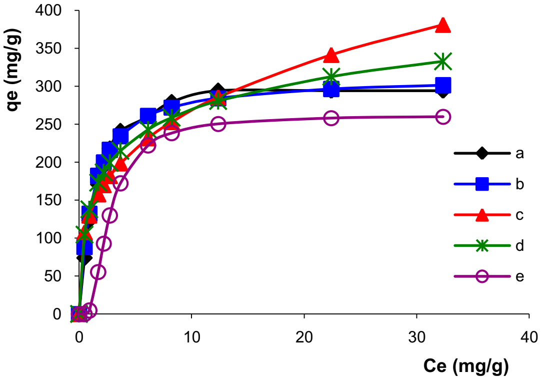

Fig. 7. Adsorption isotherm of MB onto MS002-1: (a) experimental, (b) Langmuir fit, (c) Freundlich fit, (d) Temkin fit and (e) D–R fit.

The free energy of E was calculated according to Eq. (15) and was illustrated in Table 2. The E values are 1.56 for raw clay (MS001-2) and 1.68 kJ/mol for sodium clay (MS002-1). They are orders of a physical process, in which the sorption energy lies within 1–8 kJ/mol [39–41].

4. Conclusion

In this study, the ability of local clay to bind MB was investigated using kinetic study, the pseudo-second-order kinetic model was found to be well suited for the entire adsorption process of MB on clay (MS001-2 and MS002-1). Equilibrium data fit perfectly with Langmuir isotherm model compared to Freundlich, Temkin and D–R isotherm models. The Langmuir model coefficients implied that the adsorption of MB onto minerals matrices is favourable. The overall results show that locally clay obtained from Oued Tfal-Gafsa could be used as an efficient low-cost adsorbent for dyes adsorption from aqueous solutions.

References

[1] G.O. El-Sayed, Removal of methylene blue and crystal violet from aqueous solutions by palm kernel fiber, Desalination 272 (2011) 225–232.

[2] A.R. Binupriya, M. Sathishkumar, K. Swaminathan, C.S. Ku, S.E. Yun, Comparative studies on removal of congo red by native and modified mycelial pellets of Trametes versicolor in various reactor modes, Bioresour. Technol. 99 (2008) 1080–1088.

[3] V.K. Garg, R. Kumar, R. Gupta, Removal of malachite green dye from aqueous solution by adsorption using agro-industry waste: A case study of *Prosopis cineraria*, Dyes Pigm. 62 (2004) 1–10.

[4] V.K. Garg, R. Gupta, A.B. Yadav, R. Kumar, Dye removal from aqueous solution by adsorption on treated sawdust, Bioresour. Technol. 89 (2003) 121–124.

[5] C.I. Pearce, J.R. Lloyd, J.T. Guthrie, The removal of colour from textile wastewater using whole bacterial cells: A review, Dyes Pigm. 58 (2003) 179–196.

[6] J. Yu, X. Wang, P. Yue, Optimal decolorization and kinetic modeling of synthetic dyes by *Pseudomonas* strains, Water Res. 35 (2001) 3579–3586.

[7] O.J. Hao, H. Kim, P.C. Chiang, Decolorization of wastewater, Crit. Rev. Environ. Sci. Technol. 30 (2000) 449–505.

[8] M. Zhao, Z. Tang, P. Liu, Removal of methylene blue from aqueous solution with silica nano-sheets derived from vermiculite, J. Hazard. Mater. 158 (2008) 43–51.

[9] J. Yang, K. Qiu, Preparation of activated carbons from walnut shells via vacuum chemical activation and their application for methylene blue removal, Chem. Eng J. 165 (2010) 209–217.

[10] N.K. Daud, U.G. Akpan, B.H. Hameed, Decolorization of Sunzol Black DN conc. in aqueous solution by Fenton oxidation process: Effect of system parameters and kinetic study, Desalin. Water Treat. 37 (2012) 1–7.

[11] M. Ertas, B. Acemioglu, M.H. Alma, M. Usta, Removal of methylene blue from aqueous solution using cotton stalk, cotton waste and cotton dust, J. Hazard. Mater. 183 (2010) 421–427.

[12] Z. Li, P.H. Chang, W.T. Jiang, J.S. Jean, H. Hong, Mechanism of methylene blue removal from water by swelling clays, Chem. Eng. J. 168 (2011) 1193–1200.

[13] A. Ozer, G. Dursun, Removal of methylene blue from aqueous solution by dehydrated wheat bran carbon, J. Hazard. Mater. 146 (2007) 262–269.

[14] K. Rastogi, J.N. Sahu, B.C. Meikap, M.N. Biswas, Removal of methylene blue from wastewater using fly ash as an adsorbent by hydrocyclone, J. Hazard. Mater. 158 (2008) 531–540.

[15] C. Namasivayam, R. Radhika, S. Suba, Uptake of dyes by a promising locally available agricultural solid waste: Coir pith, Waste Manage. 21 (2001) 381–387.

[16] G. Mezohegyi, F.P. van der Zee, J. Font, A. Fortuny, A. Fabregat, Towards advanced aqueous dye removal processes: A short review on the versatile role of activated carbon, J. Environ. Manage. 102 (2012) 148–164.

[17] K. Mahapatra, D.S. Ramteke, L.J. Paliwal, Production of activated carbon from sludge of food processing industry under controlled pyrolysis and its application for methylene blue removal, J. Anal. Appl. Pyrolysis 95 (2012) 79–86.

[18] S. Chinwetkitvanich, M. Tuntoolvest, T. Panswad, Anaerobic decolorization of reactive dyebath effluents by a two-stage UASB system with tapioca as a cosubstrate, Water Res. 34 (2000) 2223–2232.

[19] M.K. Saad, Y. Moussaoui, A. Zaghbani, I. Mosrati, E. Elaloui, R. Ben Salem, Influence of physico-chemical treatment on the subsequent biological process treating paper industry wastewater, Water Sci. Technol. 66 (2012) 217–223.

[20] J. Panswed, S. Wongchaisuwan, Mechanism of dye wastewater colour removal by magnesium carbonate-hydrated basic, Water Sci. Technol. 18 (1986) 139–144.

[21] P.K. Malik, S.K. Saha, Oxidation of direct dyes with hydrogen peroxide using ferrous ion as catalyst, Sep. Purif. Technol. 31 (2003) 241–250.

[22] F. Banat, S. Al-Asheh, R. Zomaout, B. Qtaishat, T. Alateat, S. Almayta, Photodegradation of methylene blue dye using bentonite as a catalyst, Desalin. Water Treat. 5 (2009) 283–289.

[23] Q. Wang, S. Tian, J. Cun, P. Ning, Degradation of methylene blue using a heterogeneous Fenton process catalyzed by ferrocene, Desalin. Water Treat. 51 (2013) 5821–5830.

[24] G. Ciardelli, L. Corsi, M. Marucci, Membrane separation for wastewater reuse in the textile industry, Resour. Conserv. Recycl. 31 (2000) 189–197.

[25] A. Bhatnagar, M. Sillanpaa, Utilization of agro-industrial and municipal waste materials as potential adsorbents for water treatment: A review, Chem. Eng. J. 157 (2010) 277–296.

[26] D.A. Fungaro, M. Bruno, L.C. Grosche, Adsorption and kinetic studies of methylene blue on zeolite synthesized from fly ash, Desalin. Water Treat. 2 (2009) 231–239.

[27] I. Feddal, A. Ramdani, S. Taleb, E.M. Gaigneaux, N. Batis, N. Ghaffour, Adsorption capacity of methylene blue, an organic pollutant, by montmorillonite clay, Desalin. Water Treat. 52 (2014) 2654–2661.

[28] M.K. Saad, R. Khiari, E. Elaloui, Y. Moussaoui, Adsorption of anthracene using activated carbon and *Posidonia oceanica*, Arabian J. Chem. 7 (2014) 109–113.

[29] M. Mhamdi, H. Galai, N. Mnasri, E. Elaloui, M. Trabelsi-Ayadi, Adsorption of lead onto smectite from aqueous solution, Environ. Sci. Technol. 20 (2013) 1686–1697.

[30] B. Zohra, K. Aicha, S. Fatima, B. Nourredine, D. Zoubir, Adsorption of Direct Red 2 on bentonite modified by cetyltrimethylammonium bromide, Chem. Eng. J. 136 (2008) 295–305.

[31] M. Gautier, F. Muller, L. Le Forestier, J.M. Beny, R. Guegan, NH_4-smectite: Characterization, hydration properties and hydro mechanical behaviour, Appl. Clay Sci. 49 (2010) 247–254.

[32] C.C. Wang, L.C. Juang, C.K. Lee, T.C. Hsu, J.F. Lee, H.P. Chao, Effect of exchanged surfactant cations on the pore structure and adsorption characteristics of montmorillonite, J. Colloid Interface Sci. 280 (2004) 27–35.

[33] N.B. Douissa, L. Bergaoui, S. Mansouri, R. Khiari, M.F. Mhenni, Macroscopic and microscopic studies of methylene blue sorption onto extracted celluloses from *Posidonia oceanica*, Ind. Crops Prod. 45 (2013) 106–113.

[34] M. Kobya, Adsorption, kinetics and equilibrium studies of Cr(VI) by hazelnut shell activated carbon, Adsorpt. Sci. Technol. 22 (2003) 51–64.

[35] O. Hamdaoui, E. Naffrechoux, Modeling of adsorption isotherms of phenol and chlorophenols onto granular activated carbon part I. Two-parameter models and equations allowing determination of thermodynamic parameters, J. Hazard. Mater. 147 (2007) 381–394.

[36] M.J. Temkin, V. Pyzhev, Recent modification to Langmiur isotherms, Acta Physiochim 12 (1940) 217–222.

[37] A.O. Dada, A.P. Olalekan, A.M. Olatunya, O. dada, Langmuir, Freundlich, Temkin and Dubinin–Radushkevich isotherms studies of equilibrium sorption of Zn^{2+} unto phosphoric acid modified rice husk, J. Appl. Chem. 3 (2012) 38–45.

[38] Q.S. Liu, T. Zheng, P. Wang, J.P. Jiang, N. Li, Adsorption isotherm, kinetic and mechanism studies of some substituted phenols on activated carbon fibers, Chem. Eng. J. 157 (2010) 348–356.

[39] M.S. Onyango, Y. Kojima, O. Aoyi, E.C. Bernardo, H. Matsuda, Adsorption equilibrium modeling and solution chemistry dependence of fluoride removal from water by trivalent-cation-exchanged zeolite F-9, J. Colloid Interface Sci. 279 (2004) 341–350.

[40] H. Chen, J. Zhao, G. Dai, Silkworm exuviae—A new non-conventional and low-cost adsorbent for removal of methylene blue from aqueous solutions, J. Hazard. Mater. 186 (2011) 1320–1327.

[41] S.S. Tahir, N. Rauf, Removal of cationic dye from aqueous solutions by adsorption onto bentonite clay, Chemosphere 63 (2006) 1842–1848.